HTML ABSTRACT + LINKS

JOURNAL OF APPLIED PHYSICS **97**, 013504 (2005)

Local strain, defects, and crystallographic tilt in GaN(0001) layers grown by maskless pendeo-epitaxy from x-ray microdiffraction

R. I. Barabash,[a] G. E. Ice, and W. Liu
Metals and Ceramics and Solid State Divisions, Oak Ridge National Laboratory, Oak Ridge, Tennessee 37831

S. Einfeldt
Institute of Solid State Physics, University of Bremen, 28334 Bremen, Germany

A. M. Roskowski and R. F. Davis
Department of Materials Science and Engineering, North Carolina State University, Raleigh, North Carolina 27695

(Received 1 June 2004; accepted 1 October 2004; published online 7 December 2004)

Polychromatic x-ray microdiffraction, high-resolution monochromatic x-ray diffraction, and finite element simulations have been used to determine the distribution of strain, defects, and crystallographic tilt in uncoalesced GaN layers grown by maskless pendeo-epitaxy. An important materials parameter was the width-to-height ratio of the etched columns of GaN from which occurred the lateral growth of the wings. Tilt boundaries formed at the column/wing interface for samples with a large ratio. Formation of the tilt boundary can be avoided by using smaller ratios. The strain and tilt across the stripe increased with the width-to-height ratio. The wings were tilted upward at room temperature. © *2005 American Institute of Physics*. [DOI: 10.1063/1.1825614]

I. INTRODUCTION

GaN films grown on sapphire or SiC contain a high density (10^{10} cm^{-2}) of threading dislocations due to lattice mismatch.[1,2] These dislocations impair the performance of GaN-based light-emitting devices. Lateral epitaxial overgrowth (LEO) techniques such as pendeo-epitaxy have recently been developed which greatly reduce the density of these dislocations.[3–5] However, some of the resulting structural and morphological characteristics of the laterally grown uncoalesced GaN films cannot be explained by the elastic relief of stress achieved in these materials via a reduction in the defect density. For example, experimental results[6] and elasticity theory do not agree on how in-plane strains and dimensions of the column correlate to the tilt angle in the laterally grown material.

In the pendeo-epitaxy process, GaN wings are grown laterally from the sidewalls of GaN columns, as shown in Fig. 1(a). The tops of the columns may or may not be masked to inhibit GaN growth. When lateral growth is continued until the complete overgrowth of a mask, threading dislocations are observed to form a boundary along each edge of the mask.[7,8] This boundary is related to the crystallographic tilt of the laterally growing wings that usually accompanies all LEO techniques. In maskless pendeo-epitaxy of GaN,[9–11] growth is initiated *simultaneously* from the sidewalls and from the top surfaces of the unmasked columns, and the wing tilt depends on the *c*-axis strain in the columns.[11] The point and extended defects generated during overgrowth in both masked and maskless pendeo-epitaxy of GaN are assumed to play an important role in the formation of strains and wing tilt, as does the mismatch in the coefficients of thermal expansion between GaN and the substrate. Despite extensive characterization, the basic structure of laterally grown films, including such critical information as the direction of the wing tilt, remains controversial. The application of polychromatic x-ray microdiffraction (PXM) to this complicated problem, together with finite element (FE) simulation and high-resolution x-ray diffraction (HRXRD), has enabled us to provide detailed information on the structure of these materials.

II. EXPERIMENTAL METHODS

GaN stripes along the $[1\bar{1}00]$ direction having a rectangular cross section were etched from 1-μm-thick GaN layers grown by metalorganic vapor phase epitaxy on 0.1-μm-thick AlN buffer layers previously deposited on 6H-SiC(0001) substrates. The subsequent overgrowth process was stopped before the wings coalesced into a layer. A schematic drawing of the stripe geometry is shown in Fig. 1(a). Details of the growth process have been reported previously.[10–12]

Two samples with different GaN stripe geometries were analyzed. The respective GaN thickness, the column width, and the wing width were 1.46, 3.80, and 0.98 μm for sample 1 and 3.53, 3.46, and 1.74 μm for sample 2. Data collection with PXM was conducted on beamline ID-34-E at the Advanced Photon Source, Argonne IL. This method uses a modified Laue diffraction technique based on polychromatic radiation. It allows for true three-dimensional mapping of a crystalline phase and its orientation, elastic strain, and plastic deformation with a spatial resolution of 0.5 μm.[13–15] The polychromatic beam produces a Laue pattern in each layer of the sample that it intercepts. The superimposed Laue patterns are detected by an x-ray sensitive CCD positioned at 90° to

[a]Electronic mail: barabashr@ornl.gov

 © 2005 American Institute of Physics

Downloaded 04 Sep 2009 to 160.91.157.167. Redistribution subject to AIP license or copyright; see http://jap.aip.org/jap/copyright.jsp

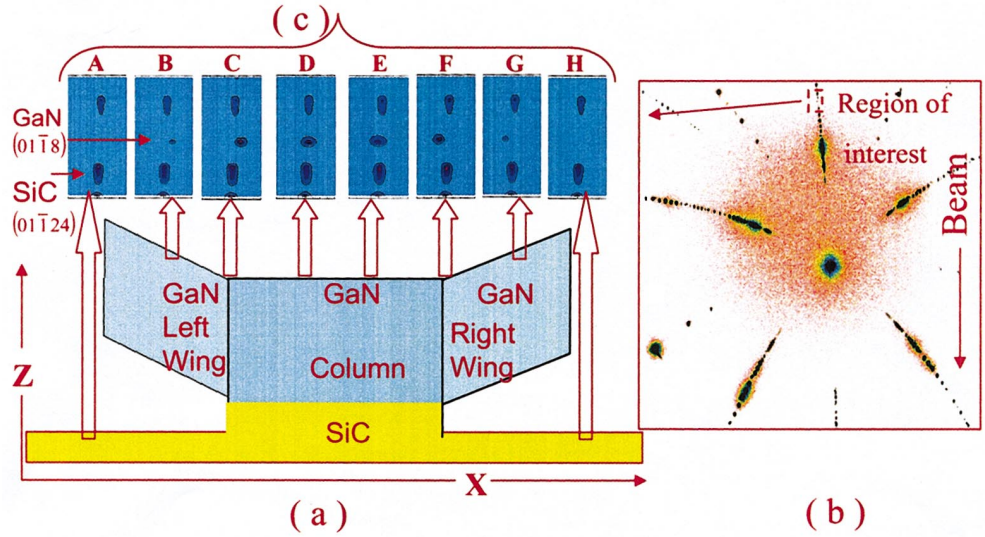

FIG. 1. (Color) (a) Scheme of the sample geometry together with a series of Laue images acquired from the region of interest showing the $(01\bar{1}8)$ GaN reflection in the center. (b) Typical Laue image showing reflections from the GaN stripe, the AlN buffer layer, and the SiC substrate. The region of interest is shown as a dashed box. (c) Laue images for sample 2 corresponding to different locations of the probe beam across the stripe: (A) SiC substrate between the wings, (B) center of the left wing, (C) left wing/column interface, (D, E) center of the column, (F) column/right wing interface, (G) center of the right wing, and (H) SiC substrate between the wings.

the incident beam. Further details regarding the experimental setup and the methods of data collection can be found elsewhere.[13–15]

HRXRD measurements were performed using a Philips X'Pert MRD diffractometer equipped with a fourfold Ge(220) monochromator and a threefold Ge(220) analyzer. Two-dimensional FE simulations were conducted as described in Ref. 11.

III. RESULTS AND DISCUSSION

A typical PXM image of GaN and SiC recorded with the diffraction plane parallel to the GaN stripe direction is shown in Fig. 1(b). The sample Cartesian reference frame is set such that the X axis is perpendicular to the stripe in the plane of the GaN film in the $\lfloor 11\bar{2}0 \rfloor$ direction. The Y axis coincides with the $\lfloor 1\bar{1}00 \rfloor$ direction of the GaN stripe, and the Z axis coincides with the [0001] direction (surface nominal normal) for both GaN and SiC. In this coordinate system the beam is incident on the surface at $\sim 45°$ with components $(0, -1/\sqrt{2}, -1/\sqrt{2})$. Diffraction patterns were collected from different sample locations by translating the sample under the white microbeam. Laue patterns were recorded along a line parallel to the sample X axis at 1000 different points with a spacing of 0.25 μm. Approximately 10–20 parallel line scans were recorded with a spacing of 0.25 μm along the Y axis to obtain a two-dimensional map of the sample. The small size of the microbeam allowed one to obtain separate images from different locations on the column and the wings. Because the high-energy x-ray beam passed through the GaN and the AlN layers, the SiC substrate contributed to the observed Laue patterns; the reflections originating from the SiC were superimposed on those from the GaN for all the PXM images. A small region of interest from typical PXM images is enlarged in Fig. 1(c) to clearly show the behavior of the SiC and the GaN reflections at different locations along the X direction. The region of interest within the larger Laue pattern is shown as a dashed square in Fig. 1(b). This region

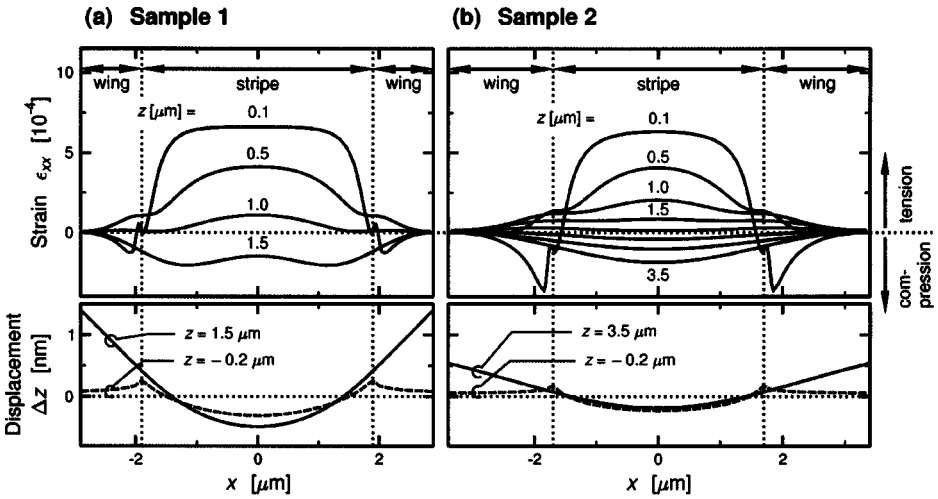

FIG. 2. Line scans of the normal strain in GaN along the X axis for different Z values (upper part) and the displacement along the Z axis (lower part) as determined from FE simulations for samples 1 and 2, respectively. The height $Z=0$ corresponds to the GaN/SiC interface.

Downloaded 04 Sep 2009 to 160.91.157.167. Redistribution subject to AIP license or copyright; see http://jap.aip.org/jap/copyright.jsp

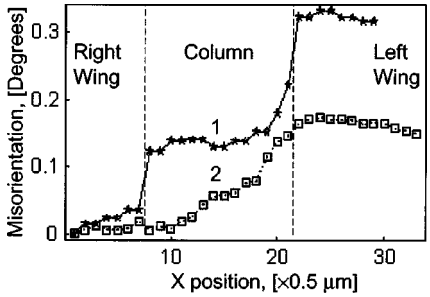

FIG. 3. Relative crystallographic orientation of the GaN *c* axis across the stripe as determined from PXM analysis for samples 1 and 2, respectively.

belongs to a vertical zone line with the zone axis running along the *X* direction. Two Laue reflections associated with SiC and one reflection associated with GaN are present within the region of interest. The SiC reflections do not change position with sample translation and can be easily identified within the images A and H of Fig. 1(c), where only the SiC is probed (the region between two adjacent wings). The SiC Laue reflections were used as a reference to determine the position of the GaN$(01\bar{1}8)$ Laue reflection. When the probe spot is moved along the positive *X* axis and initially encounters the left wing, the GaN reflection appears at the right side of the SiC reflections, as shown in image B of Fig. 1(c). As the probe spot is moved across the wing to the wing/column interface one GaN reflection from the wing and one from the column can be observed, as shown in image C of Fig. 1(c). When the probe is in the center of the column, the GaN reflections are aligned with the SiC reflections, as shown in images D and E of Fig. 1(c). With further displacement towards the right wing, the GaN reflections appear to the left of the SiC reflections, as shown in images F and G of Fig. 1(c). The GaN reflection finally disappears when the probe spot is again between wings, as shown in image H of Fig. 1(c). The shift of the GaN reflections along with the geometry of the structure shown in Fig. 1(a), clearly indicates that the wings are tilted upward. This was confirmed by physically tilting the sample to ensure that the CCD image was consistent with the applied inclination of the sample.

An upward tilt of the wings is also predicted by the results of FE simulations shown in Fig. 2. For these calculations it was assumed that the GaN is under biaxial tensile stress in the *c* plane due to the mismatch in the coefficients of thermal expansion between the GaN layer and the SiC substrate. The stress in the *X* direction is increasingly relieved towards the GaN surface as the uncoalesced GaN layer contracts laterally. The inhomogeneous stress relief results in the inclination of the stripe/wing interface plane and, consequently, in the upward tilt of the wings. Further explanation of this process can be found in Ref. 11.

PXM for samples with minimal deformation has an angular resolution of $<0.01°$. This makes it possible to quantitatively determine the GaN tilt as a function of distance from the column, as shown in Fig. 3. The maximum tilt of the wings relative to the center of the column is $\sim 0.16°$ for sample 1 and $\sim 0.08°$ for sample 2. In Laue diffraction, the directions of the incident beam and the scattered beam define a radial line in reciprocal space. The position along this line is determined by the wavelength of the scattered radiation.

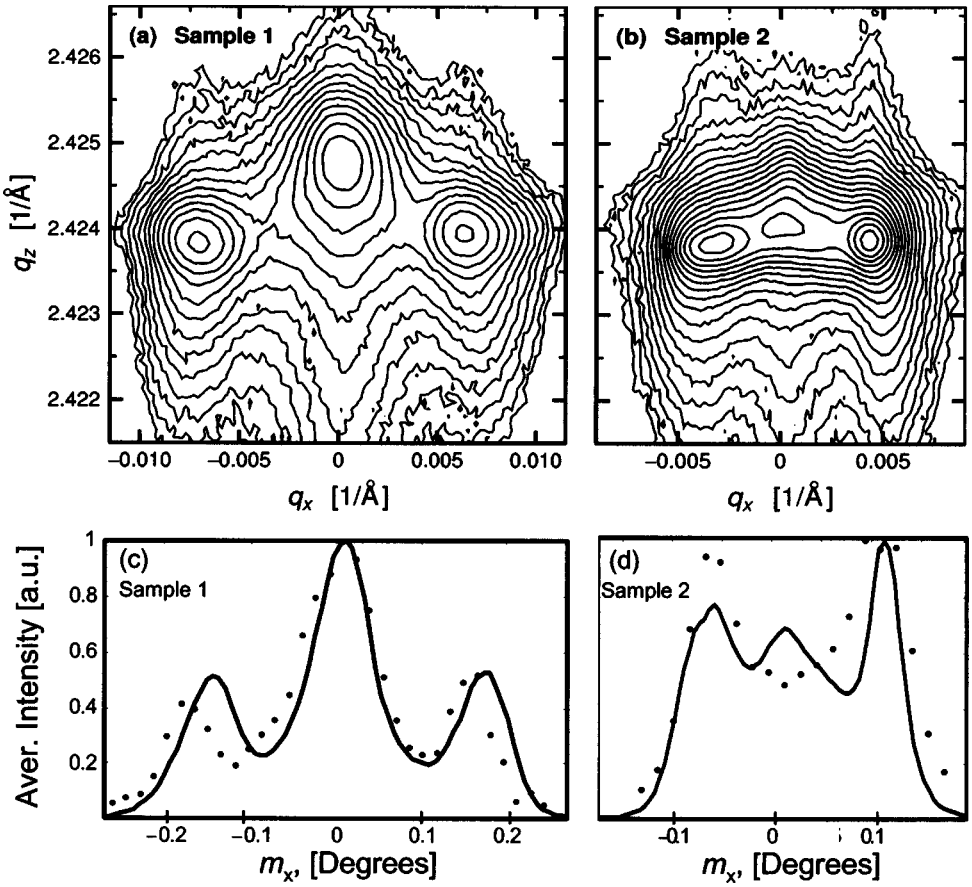

FIG. 4. HRXRD reciprocal space maps of the GaN(0002) reflection and the average intensity profiles versus the *X* component of misorientation vector m_x for samples 1 (a) and 2 (b). Laue intensity distribution averaged along the stripe direction for samples 1 (c) and 2 (d), as determined by PXM as a function of the misorientation vector $\boldsymbol{m}$ in the $[11\bar{2}0]$ direction perpendicular to the stripes (dots) and averaged along the *Z*-direction rocking curve intensity (solid lines).

Downloaded 04 Sep 2009 to 160.91.157.167. Redistribution subject to AIP license or copyright; see http://jap.aip.org/jap/copyright.jsp

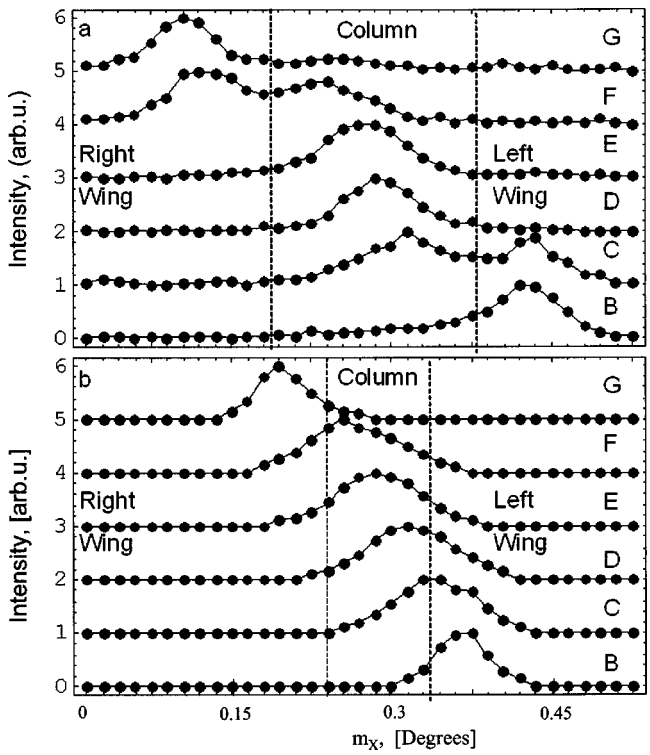

FIG. 5. PXM intensity profiles through the GaN$(01\bar{1}8)$ Laue reflection as a function of m_x at different locations across the stripe for sample 1(a) and sample 1(b). The locations B–G are defined in Fig. 1.

For example, the reciprocal lattice points (00*h*), (002*h*), (003*h*), etc. are scattered towards the same pixel on a CCD but lie at different positions radially in reciprocal space. To analyze the white beam intensity distribution from a GaN stripe, we introduced unit vectors $\hat{\mathbf{k}}=\mathbf{k}/|\mathbf{k}|$, in each direction of scattering. We defined a misorientation vector $\mathbf{m}=\hat{\mathbf{k}}-\hat{\mathbf{k}}_{hkl}$ near a Bragg (*hkl*) reflection, the value of which is the difference between the unit vector parallel to the Bragg reflection and an arbitrary direction in its vicinity.[15] The results from the PXM studies are shown in Figs. 3–6 as a function of $\mathbf{m}$ in the $\lfloor 11\bar{2}0 \rfloor$ direction; that is, perpendicular to GaN stripe.

The results of PXM are in agreement with the results of HRXRD. Figure 4 contains a collection of reciprocal space maps (RSM) of the (0002) GaN reflection obtained by HRXRD for both samples with the diffraction plane being perpendicular to the stripes. Three peaks can be found, which correspond to the left wings, the columns, and the right wings, respectively. The separation of the peaks along the q_x axis reflects the different orientation of the *c* axis of the three regions; that is, the wing tilt. The corresponding values extracted from these measurements are 0.159° and 0.085° for samples 1 and 2, respectively. It is worth noting that in HRXRD the spot size of the x-ray beam is large (~0.5 mm); that is, the value of the RSM gives information averaged over thousands of stripes. In contrast, PXM provides very local information and enables us to follow the local orientation at different locations across the stripe. For a clearer comparison to the HRXRD results, the Laue intensity profiles averaged over different locations of the probe spot

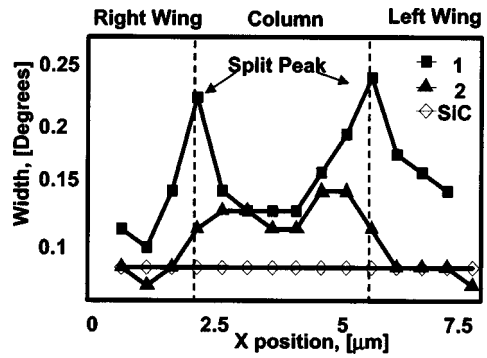

FIG. 6. Width of the GaN$(01\bar{1}8)$ Laue reflection at $0.3I_{max}$ across the GaN stripe as determined from PXM images. The width of the nearest $(01\bar{1}24)$ SiC reflection is shown for comparison (filled squares: sample 1, filled triangles: sample 2, open diamonds: SiC).

with respect to the column are presented by dots in Figs. 4(c) and 4(d). Rocking curve profiles, obtained by averaging all the ω-scans recorded for the RSM, are also shown in Figs. 4(c) and 4(d) by solid lines. The good agreement between HRXRD and PXM suggests that the wing tilt is quite homogeneous across the samples.

FE simulations predict an increase in the wing tilt with an increasing width-to-height ratio of the column.[11] This is in agreement with the experimental data. Sample 1 has a width-to-height ratio of the column of 2.60 and a wing tilt of 0.16°, whereas the corresponding numbers for sample 2 are 0.98 and 0.08°, respectively. Moreover, the PXM data presented in Fig. 3 reveals that the crystallographic tilt changes abruptly at the column/wing interface for sample 1. However, this change is more gradual in sample 2 and extends over the whole column between the right and left wing. This is also consistent with FE simulations, which predict that if the width-to-height ratio of the column decreases, the wing tilt should change more gradually across the stripe.

Broadening of the GaN Laue reflections along the m_x direction can be analyzed at corresponding intensity profiles through the PXM images, as shown in Fig. 5. The intensity profiles for both samples are labeled in Fig. 5 in correspondence with the position of the probed locations on the stripe shown in Fig. 1(a). A comparison of the PXM results from samples 1 and 2 shows that the broadening is generally more pronounced for sample 1; that is, the sample with the larger width-to-height ratio of the GaN column. Moreover, the reflection corresponding to the column is more broadened than the reflection corresponding to the wing, as can be seen, for example, when comparing the intensity profiles D and G in Fig. 5(b). The ratios of the corresponding peak widths are approximately 1.2±5% and 1.9±10% for samples 1 and 2, respectively. Similar results are obtained from the HRXRD (0002) rocking curves. The ratios of the peak widths for the column and wing are unity and three for samples 1 and 2, respectively. The intensity profiles in Fig. 5(a) for sample 1 show that the GaN reflection is particularly broadened at the column/wing interface where it splits into two distinct peaks [compare curves C and F in Fig. 5(a)]. It should be noted that it is this sample for which the wing tilt changes abruptly at this interface, as was shown in Fig. 3. This indicates that a

Downloaded 04 Sep 2009 to 160.91.157.167. Redistribution subject to AIP license or copyright; see http://jap.aip.org/jap/copyright.jsp

small angle tilt boundary has formed at the column/wing interface in sample 1. For sample 2 (with the smaller width-to-height ratio of the GaN column), however, this seems not to be the case. Figure 5(b) shows that the crystallographic orientation gradually changes across the stripe for this sample, as shown in Fig. 3. The width of the column peak obtained by HRXRD for sample 2 is much higher than the broadening measured by PXM at each local position within the column due to the orientation spread in the column.

It has been reported previously,[12] that GaN layers mimic the domain tilt of the substrate when grown on 6H-SiC (0001) wafers. Therefore, the broadening of the Laue reflections of GaN and SiC in the m_x direction across the stripe is plotted together in Fig. 6. The Laue spot width was determined at the level of 0.3 $I_{\max}$ for both samples in order to include the broadening of the bimodal intensity profile appearing in some intensity scans. The width of the SiC Laue reflection remains the same at all locations, as shown by the corresponding horizontal line in Fig. 6. The GaN Laue reflections in the region of the column are always broader than the SiC reflections. This indicates that the broadening of the GaN reflection in this region *is not* due to imperfections of the substrate but arises mainly due to defects such as threading dislocations and to an inhomogeneous crystallographic orientation within the column, in agreement with the FE simulations (Fig. 2). In comparison to the column, the width of the GaN reflections from the wing regions are much smaller for both samples, and are about the same as the widths of the SiC reflections. This confirms that the density of defects and the inhomogeneity of the strain are reduced in the wings as compared to the column.

IV. SUMMARY

X-ray PXM experiments have unambiguously shown that the crystallographic tilt of the wings in GaN layers grown on SiC substrates by maskless pendeo-epitaxy is upward. This is consistent with FE simulations that assume the elastic relief of thermally induced tensile stress in the GaN. The distribution of the tilt across the stripe depends on the width-to-height ratio of the column and on the thickness of the overgrown GaN layer. For small width-to-height ratios the tilt is small, and it changes gradually in the region of the column. For large width-to-height ratios the tilt is higher, and a low-angle tilt boundary is formed at the column/wing interface. The dislocation density was reduced and/or the strain was more homogeneous in the wings than in the columns.

ACKNOWLEDGMENTS

The authors wish to thank Detlef Hommel (University of Bremen, Germany) for encouragement and useful suggestions of this work. The research was supported in part by the U. S. Department of Energy, Division of Materials Sciences and Engineering through a contract with the Oak Ridge National Laboratory. Oak Ridge National Laboratory (ORNL) is operated by UT-Battelle, LLC, for the U.S. Department of Energy under Contract No. DE-AC05-00OR22725. The research at NCSU was sponsored by the Office of Naval Research via contract N00014-98-1-0654 (Harry Dietrich, monitor). Measurements were performed on the Unicat beamline 34-ID at the Advanced Photon Source. The UNICAT facility at the Advanced Photon Source (APS) is supported by the U.S. DOE under Award No. DEFG02-91ER45439, through the Frederick Seitz Materials Research Laboratory at the University of Illinois at Urbana-Champaign and the Oak Ridge National Laboratory (U.S. DOE Contract No. DE-AC05-00OR22725 with UT-Battelle LLC. The APS is supported by the U.S. DOE, Basic Energy Sciences, Office of Science under Contract No. W-31-109-ENG-38. The submitted manuscript has been authored by a contractor of the U.S. Government under Contract No. DE-AC05-00OR22725. Accordingly, the U.S. Government retains a nonexclusive, royalty-free license to publish or reproduce the published form of this contribution, or allow others to do so, for U.S. Government purposes.

[1] S. D. Lester, F. A. Ponce, M. G. Craford, and D. A. Steigerwald, Appl. Phys. Lett. **66**, 1249 (1995).
[2] T. Metzger, R. Hopler, and E. Born, Philos. Mag. A **77**, 1013 (1998).
[3] S. Einfeldt, Z. J. Reitmeier, and R. F. Davis, J. Cryst. Growth **253**, 129 (2003).
[4] O.-H. Nam, M. D. Bremser, T. S. Tsvetanka, and R. F. Davis, Appl. Phys. Lett. **71**, 2638 (1997).
[5] K. Linthicum, T. Gehrke, D. Thomson, E. Carlson, P. Rajagopal, T. Smith, D. Batchelor, and R. Davis, Appl. Phys. Lett. **75**, 196 (1999).
[6] S. Einfeldt, D. Hommel, and R. F. Davis, *Strain in GaN Layers Grown by Metalorganic Vapor Phase Epitaxy*, in Vacuum Science and Technology: Nitrides as Seen by the Technology, edited by T. Paskova and B. Monemar (Research Signpost, Kerela, India, 2003), pp. 147–166.
[7] A. Sakai, H. Sunakawa, and A. Usui, Appl. Phys. Lett. **73**, 481 (1998).
[8] H. Marchand, X. H. Wu, J. P. Ibbetson, P. T. Fini, P. Kozodoy, S. Keller, J. S. Speck, S. P. DenBaars, and U. K. Mishra, Appl. Phys. Lett. **73**, 747 (1998).
[9] T. S. Zheleva, S. A. Smith, D. B. Thomson, T. Gehrke, K. J. Linthicum, P. Rajagopal, E. Carlson, W. Ashmawi, and R. F. Davis, MRS Internet J. Nitride Semicond. Res. **4S1**, G3.38 (1999).
[10] A. M. Roskowski, P. Q. Miraglia, E. A. Preble, S. Einfeldt, T. Stiles, R. F. Davis, J. Schuck, R. Grober, and U. Schwarz, Phys. Status Solidi A **188**, 729 (2001).
[11] S. Einfeldt, A. M. Roskowski, E. A. Preble, and R. F. Davis, Appl. Phys. Lett. **80**, 953 (2002).
[12] R. F. Davis, S. Einfeldt, E. A. Preble, A. M. Roskowski, Z. J. Reitmeier, and P. Q. Miraglia, Acta Mater. **51**, 5961 (2003).
[13] J. Budai, W. Yang, N. Tamura, J.-S. Chung, J. Tischler, B. Larson, G. Ice, C. Park, and D. Norton, Nat. Mater. **2**, 487 (2003).
[14] R. Barabash, G. Ice, B. Larson, G. Pharr, K. Chung, and W. Yang, Appl. Phys. Lett. **79**, 749 (2001).
[15] R. Barabash, G. Ice, and F. Walker, J. Appl. Phys. **93**, 1457 (2003).

Downloaded 04 Sep 2009 to 160.91.157.167. Redistribution subject to AIP license or copyright; see http://jap.aip.org/jap/copyright.jsp